JJBS

Jordan Journal of Biological Sciences

Volume 12, Number 2,June 2019
ISSN 1995-6673
Pages 183 - 189

Virtual Screening for Inhibitors Targeting the Rod Shape-Determining Protein in *Escherichia coli*

Mohammed Z. Al-Khayyat[1*], Ammar Gh. Ameen[2] and Yousra A. Abdulla[1]

[1]*Biology Department, College of Education for Pure Sciences,* [2] *Biology Department, College of Science, University of Mosul, Mosul city, Iraq*

Received June 20, 2018; Revised August 26, 2018; Accepted August 28, 2018

Abstract

The rod shape-determining protein, MreB, is a bacterial actin analog and is involved in determining the shape of non-spherical bacteria. A tertiary structure of MreB from *Escherichia coli* was constructed by an online server, RaptorX, and its accuracy was assessed by four validation tools. The docking software, AutoDock Vina was used to dock a total of one-hundred natural occurring compounds obtained from ZINC and PubChem databases. The pharmacokinetics and toxicity profiles of the compounds were predicted by Swiss ADME tool. The results indicate that amentoflavone, rutin, and chlorogenic acid had binding affinities of -10.9, -10.1 and -9.3 Kcal/mol respectively which were higher than the control, ATP, -9.2 Kcal/mol. In the pharmacokinetic profiling, these three compounds were not inhibitors of cytochromes, but had a low gastrointestinal absorption. MreB may serve as an alternative molecular target for new antibiotics against rod-shape resistant microbes, since the disruption of its function may lead to bacterial cell lysis.

Keywords: Amentoflavone, AutoDock Vina, Docking, Homology modeling, MreB.

1. Introduction

The rod shape-determining protein, MreB, is a component of bacterial cytoskeleton, and is an analog of the eukaryotic actin. MreB is a product of *mre* operon (murein gene cluster e) (Doi *et al*., 1988). Unlike actin, MreB uses ATP to polymerize into helical filaments encircling the whole cell just under the cytoplasmic membrane (Jones *et al.*, 2001). This activity is essential for maintaining the rod shape of *Escherichia coli*, *Caulobacter crescentus*, and *Thermotoga maritime* (Salje *et al.*, 2011). Several proteins act for this purpose in non-spherical bacteria including two membrane proteins encoded by *mreC* and *mreD*. The cell wall biosynthetic component, Penicillin-binding protein 2 (PBP2), via interaction with MreC also participates in the process (Wachi *et al.*, 1989; Slovak *et al.*, 2006; van den Ent *et al.*, 2010). Another cell protein, RodZ, interacts with of MreB in the process of cell wall synthesis by affecting its biophysics. The expression of these two proteins varies in response to cell width and growth rate variations (Colavin *et al*., 2018). Mutagenesis of *mreB* results in the loss of the normal rod-shape of *E. coli* and the formation of spherical cells. These slowly growing irregular cells are hypersensitive to antibiotics targeting cell wall synthesis such as mecillinam, and tend to lyse under normal growth conditions (Wachi *et al*., 1987; Bendezú and de Boer, 2008).

The failure of the currently-used antimicrobials to combat infections caused by resistant microbes encouraged researchers to search for new molecular targets upon which newer agents may work either to kill pathogenic microbes or eliminate their pathogenicity. A suggested approach is to screen libraries of natural or synthetic compounds capable of binding a selected molecular targets inside the bacterial cell. A selected compound should be able to abolish the function of this selected target. Docking experiments may be used to compute *in silico* the binding affinity of ligands with the molecular targets, and present the results in a scoring system (Allsop and Illingworth, 2002; Huang and Zou, 2010).

Due to difficulties in the purification of this protein, most structural studies of MreB were conducted on *T. maritima* because there is no experimental structure that has been determined for *E. coli* (Salje *et al.*, 2011). The only study of the MreB inhibition, is that of Iwai *et al*. (2002) in which the compound S-(3,4-dichlorbenzyl) isothiourea, affected MreB of *C. crescentus*, and resulted in converting the rod-shape cells into spherical ones (Iwai *et al.*, 2002).This study is aimed at building a model of *E. coli* MreB, and carrying out docking experiments in order to find possible inhibitors.

2. Materials and Methods

2.1. Homology Modeling

The amino-acid sequence of MreB (Doi *et al.*, 1988) was obtained from Uniprot database which can be accessed at http://www.uniprot.org/. The MreB accession number was (P0A9X4). The protein tertiary structure was built by an online server, RaptorX (Källberg *et al*., 2112), at (http://raptorx.uchicago.edu/) which also predicts the

* Corresponding author e-mail: mzsaeed19@hotmail.com.

binding site. The sequence was visualized by BioEdit 3.3.19.0 (Hall, 1999). The three-dimensional structure was visualized by ArgusLab 4.0.1 (Thompson, 2004) and for the protein-ligand interactions, LigPlot^{+} was used (Wallace *et al*., 1996).

2.2. Quality Assessment of the Model

The accuracy of the model was assessed by four online tools; (a) ERRAT (Colovos and Yeates, 1993) at (http://services.mbi.ucla.edu/ERRAT/), (b) PROSA (Sippl, 1993; Wiederstein and Sippl, 2007), accessed at (https://prosa.services.came. sbg.ac.at/prosa.php), (c) Qualitative Model Energy Analysis tool, QMEAN6 (Benkert *et al.*, 2009) at: (https://swissmodel.expasy.org/); (d) Ramachandran plot analysis by RAMPAGE *(*Lovell *et al.*, 2002*),* at (http://mordred.bioc.cam.ac.uk/~rapper/ rampage. php). The model was submitted into the protein model database (PMDB) (Castrignano *et al.*, 2006) which can be accessed at http://bioinformatics.cineca.it/ PMDB.

2.3. Molecular Docking

A total of one-hundred natural compounds were obtained from ZINC database (Irwin *et al.*, 2012) available at (http://zinc.docking.org/) and PubChem database (Kim *et al.*, 2016) available at (http://pubchem.ncbi.nlm.nih.gov). These two databases also provide the molecular properties: mass, H-bond donors, H-bond acceptors, and polar surface area. Molecular docking was performed using AutoDock Vina (Trott and Olson, 2010). The Autogrid tool was employed to pre-calculate a grid. This grid has a size of 60×60×60 and a box center of 1.615,-1.708 and 22.49 for x, y, and z respectively.

2.4. Pharmacologic Properties of the Compounds

The pharmacokinetics of the compounds were predicted by Swiss ADME (Daina *et al.*, 2017) at http://www.swissadme.ch/. The computed parameters were: (1) Gastro-intestinal absorption (GI absorption), (2) blood-brain barrier (BBB) penetration, (4) plasma glycoprotein (P-gp) substrate and (5) Cytochromes (CYP P_{450}), inhibition.

3. Results

The constructed model (Figure 1) appears to be composed of 40 % α-helices, 25 % β-strands and 36 % as coils. Since there is no experimental structure of MreB for *E. coli*, the selected template was 2 Å X-ray crystal structure of rod shape-determining protein of *C. crescentus* (Löwe and van den Ent, 2014). This template has a PDB ID of 4cze.1A with a sequence identity of 63.75 % and 95 % coverage of the predicted model. The predicted model was submitted onto protein model database with PMDB ID: PM0080558. The constructed model of MreB has the following topology: β1 $D^{12}\rightarrow G^{18}$, β2 $A^{20}\rightarrow V^{26}$, β3 $G^{30}\rightarrow D^{36}$,β4 $V^{38}\rightarrow R^{45}$, β5 $S^{48}\rightarrow G^{56}$, α1 $H^{57}\rightarrow Q^{61}$, β6 $N^{69}\rightarrow K^{77}$, α2 $F^{84}\rightarrow V^{98}$, β7 $R^{109}\rightarrow V^{114}$, α3 $Q^{120}\rightarrow A^{133}$, β8 $E^{137}\rightarrow I^{141}$, α4 $P^{144}\rightarrow I^{149}$, β9 $S^{161}\rightarrow G^{167}$, β10 $T^{170}\rightarrow S^{177}$, β11 $G^{180}\rightarrow V^{187}$, α5 $G^{191}\rightarrow Y^{206}$, β12 $G^{207}\rightarrow L^{209}$, α6 $E^{212}\rightarrow I^{222}$, β13 $R^{232}\rightarrow L^{241}$, β14 $V^{245}\rightarrow S^{253}$, α7 $N^{254}\rightarrow A^{276}$, α8 $P^{280}\rightarrow R^{289}$, β15 $M^{291}\rightarrow T^{294}$, α9 $L^{303}\rightarrow T^{311}$, β16 $I^{314}\rightarrow A^{318}$ and α10 $P^{321}\rightarrow L^{333}$.

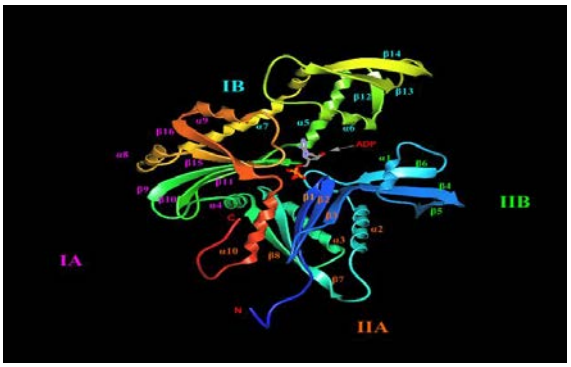

Figure 1. The MreB model as predicted by RaptorX. Numbering starts from N-terminal towards (N) to C-terminal (C). MreB monomer consists of two domains I and II. Subdomain IA and IIA have the topology of five β-sheets surrounded by three α-helices, while the smaller subdomains are variable. Subdomain IA comprises α4, α8, β9, β10, β11, β15, β16 and α9 while subdomain IIA comprises α2, α3, β1, β2, β3, β7, β8 andα10. The variable smaller subdomain IB comprises α5, α6, β12, β13, β14 andα7and while subdomain IIB comprises α1, β4, β5 and β6. ADP occupies a cleft between domains I and II where its phosphate groups interact. These two sub-domains are connected via a helix, α4.

RaptorX predicted two binding sites of the model. The largest pocket is for ADP molecule and consists of following residues: G^{18}, T^{19}, A^{20}, N^{21}, G^{167}, G^{168}, G^{169}, G^{191}, E^{216}, K^{219}, H^{220}, G^{295}, G^{296}, G^{297}, L^{299}, L^{300} and L^{322}. A second smaller pocket was predicted for binding Mg^{+2} ion, which is composed of E^{143} and D^{165} (Figure 2).

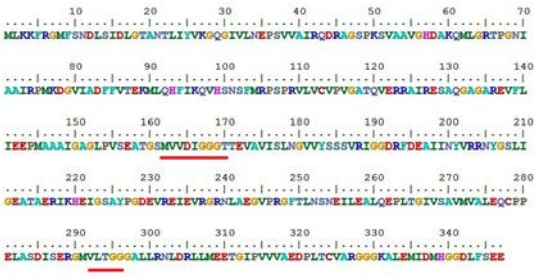

Figure 2. Amino acid sequence of MreB (Doi *et al.*,, 1988). ATP binding motifs are marked with a red underline.

Four evaluation tools were used to measure the accuracy of the model. ERRAT overall quality of the model is 88.855 % (Figure 3 A). PROSA Z-score is -10.66 (Figure3 B). The raw score of QMEAN6 is 0.713 which is in the normal range of 0-1. A comparison of Z-scores with experimentally determined structures is shown in (Figure 3 C). In the Ramachandran plot analysis, the constructed MreB model has 338(98.0 %) of the residues being in the favored region (Figure 4), and three residues (0.9 %) in the allowed region. These residues are S^{102}, V^{231} and M^{335}. Four residues (1.2 %) were in the disallowed (outlier) region. These residues are R^{45}, N^{101}, F^{103} and D^{229}.

A total of one-hundred natural compounds were docked against the predicted model; the highest ten are shown in Table 1. Figure 5 shows ATP at its binding site in MreB and the interaction with the MreB amino acid residues. The results of AutoDock Vina show that there are three compounds, namely amentoflavone, rutin, and chlorogenic acid which had higher binding affinities than ATP. Figures 6-8 show the docking of the three ligands against MreB

and the amino-acid residues involved. Figure 9 shows the chemical structure of these three compounds.

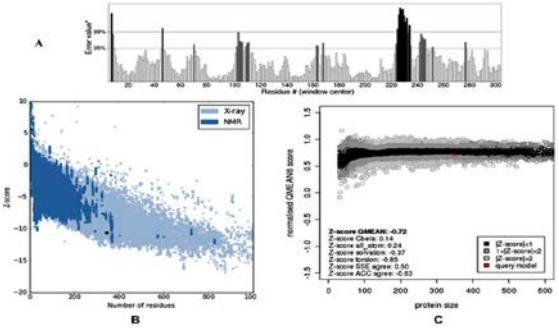

Figure 3. (A) ERRAT result of the generated model. Black bars represent misfolded regions. On the error axis two lines are drawn to indicate the confidence in which it is possible to reject regions (B) Z-score of MreB (black dot) computed by PROSA web tool compared with Z-scores of the experimentally determined proteins by NMR spectroscopy and X-ray crystallography (C) QMEAN6 plot of MreB model showing a comparison with-non redundant set of known experimental PDB structures in Z-scores.

Figure 4. Ramachandran plot of the predicted model using RAMPAGE. Residues in the disallowed regions are red-colored

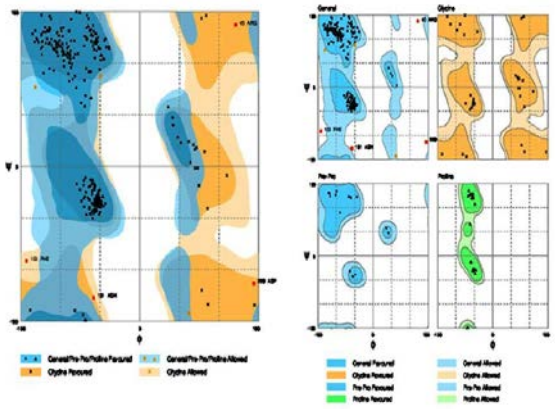

squares, while residues in the allowed region are brown-colored squares.

Table 1. Results of docking *E. coli* MreB

Compound	Database ID	Binding affinity (Kcal/mol)	Residues forming hydrogen bonds	Residues forming hydrophobic interactions
ATP	ZINC18456332	-9.2	D^{16}, N^{21}, E^{143}, D^{165}, G^{168}, G^{192}, G^{195}	A^{20}, G^{167}, G^{191}, K^{219}, H^{220}, G^{295}, L^{299}, L^{322}
Amentoflavone	ZINC03984030	**-10.9**	D^{16}, N^{21}, E^{143}, G^{168}	G^{18}, T^{19}, A^{20}, G^{167}, F^{194}, K^{219}, H^{220}, G^{295}, G^{296}, L^{299}, L^{300}, L^{322}, V^{325}
Rutin	ZINC59764511	**-10.1**	D^{16}, R^{74}, D^{165}, G^{168}, G^{296}, G^{297}, L^{322}	G^{18}, A^{20}, N^{21}, N^{34}, E^{35}, P^{36}, K^{60}, E^{143}, G^{167}, G^{191}, D^{195}, E^{216}, K^{219}, H^{220}, G^{295}, V^{325}
Chlorogenic acid	ZINC02138728	**-9.3**	D^{16}, T^{19}, N^{21}, E^{143}, G^{169}, T^{170}	G^{18}, A^{20}, G^{79}, D^{165}, G^{167}, G^{168}, G^{191}, G^{295}, V^{325}
Scutellarin	ZINC21902916	-9.2	D^{16}, T^{19}, G^{168}, G^{296}, L^{322}	G^{18}, A^{20}, P^{36}, N^{21}, G^{167}, G^{191}, K^{219}, G^{296}
Takakin	ZINC14813980	-8.6	D^{16}, T^{19}, E^{143}, G^{168}	G^{18}, A^{20}, N^{21}, G^{167}, D^{195}, K^{219}, G^{295}, G^{296}, L^{322}, V^{325}
Coumestrol	ZINC00001219	-8.3	-	A^{20}, G^{168}, G^{191}, K^{219}, H^{220}, G^{296}, G^{297}, L^{299}, L^{300}
Hinokinin	ZINC01872258	-8.3	-	D^{16}, A^{20}, N^{21}, K^{60}, E^{143}, I^{166}, G^{167}, G^{168}, G^{191}, D^{195}, E^{216}, E^{216}, K^{219}, H^{220}, G^{296}, G^{297}, L^{322}
Bucegin	ZINC14757469	-8.3	G^{191}	A^{20}, N^{21}, G^{167}, G^{168}, K^{219}, H^{220}, G^{223}, G^{296}, G^{297}, L^{299}, L^{300}, R^{301}, L^{322}
Isoquercitrin	ZINC04096845	-8.2	I^{166}, D^{195}, K^{219}	A^{20}, N^{21}, N^{34}, E^{35}, P^{36}, K^{60}, G^{167}, G^{168}, G^{191}, E^{216}, H^{220}, G^{296}, G^{297}, L^{322}
Vitexin	ZINC04339745	-8.1	D^{192}	A^{20}, N^{21}, G^{168}, G^{191}, F^{194}, D^{195}, E^{216}, K^{219}, H^{220}, G^{296}, G^{297}, L^{299}, L^{300}, L^{322}

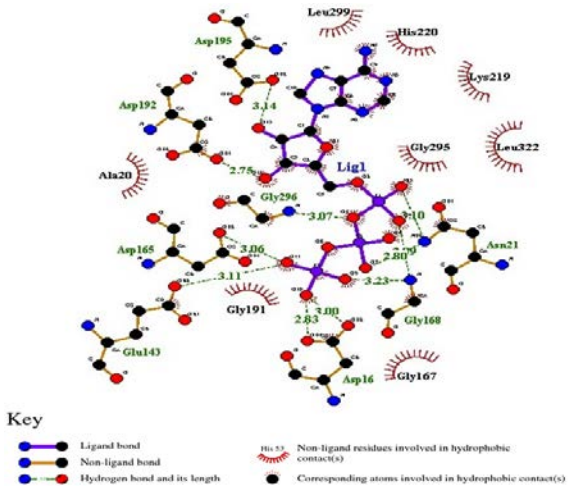

Figure 5. ATP interaction with MreB. ATP forms H-bonds with the amino-acid residues D^{16} (2.83, 3.00 A°), N^{21} (3.10, 2.09 A°), E^{143} (3.11 A°), D^{165} (3.06 A°), G^{168} (2.80, 3.23 A°), G^{192} (2.75 A°) and G^{195} (3.14 A°). ATP also has hydrophobic interactions with A^{20}, G^{167}, G^{191}, K^{219}, H^{220}, G^{295}, L^{299} and L^{322}.

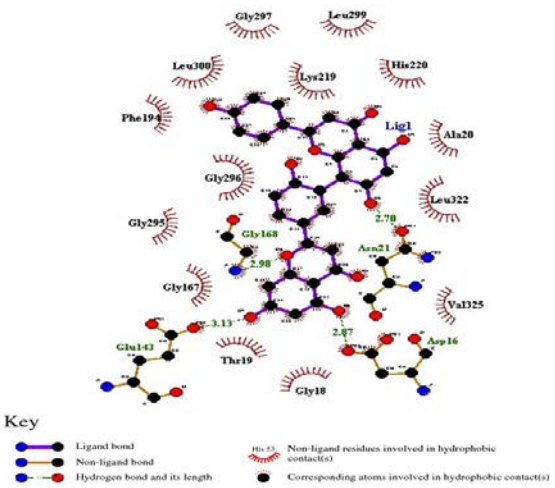

Figure 6. Amentoflavone interaction with MreB. Amentoflavone forms H-bonds with the amino-acid residues D^{16} (2.87 A°), N^{21} (2.70 A°), E^{143} (3.13 A°) and G^{168} (2.98 A°). It also has hydrophobic interactions with G^{18}, T^{19}, A^{20}, G^{167}, F^{194}, K^{219}, H^{220}, G^{295}, G^{296}, L^{299}, L^{300}, L^{322}, and V^{325}.

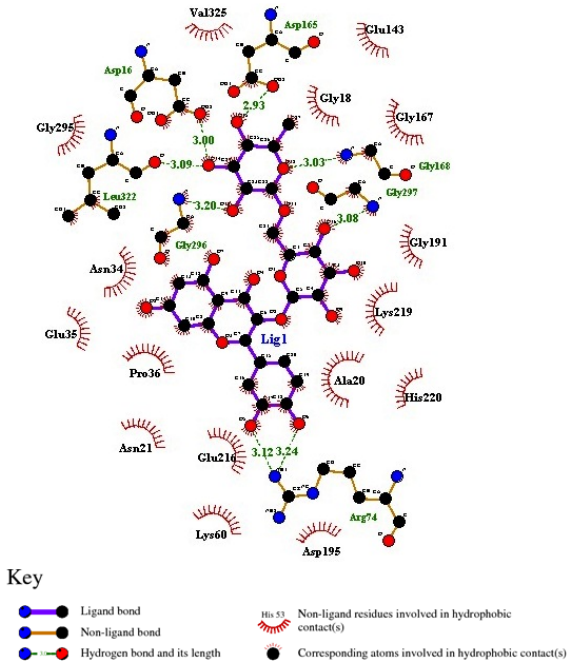

Figure 7. Rutin interaction with MreB. Rutin forms H-bonds with the amino-acid residues D^{16} (3.00 A°), R^{74} (3.12, 3.24 A°), D^{165} (2.93 A°), G^{168} (3.03 A°), G^{296} (3.20 A°), G^{297} (3.08 A°) and L^{322} (3.09 A°). It also has hydrophobic interactions with G^{18}, A^{20}, N^{21}, N^{34}, E^{35}, P^{36}, K^{60}, E^{143}, G^{167}, G^{191}, D^{195}, E^{216}, K^{219}, H^{220}, G^{295}, and V^{325}.

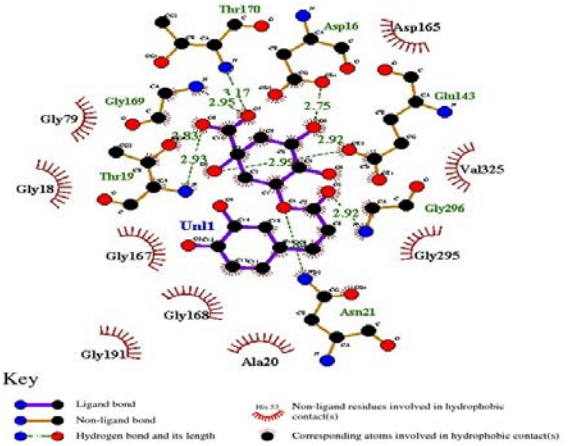

Figure 8. Chlorogenic-acid interaction with MreB. Chlorogenic acid forms H-bonds with the amino-acid residues D^{16} (2.75 A°), T^{19} (2.83, 2.93 A°), N^{21} (2.84 A°), E^{143} (2.99, 2.92 A°) and G^{169} (2.95 A°), T^{170} (3.17 A°) and G^{296} (2.92 A°). It also has hydrophobic interactions with G^{18}, A^{20}, G^{79}, D^{165}, G^{167}, G^{168}, G^{191}, G^{295} and V^{325}.

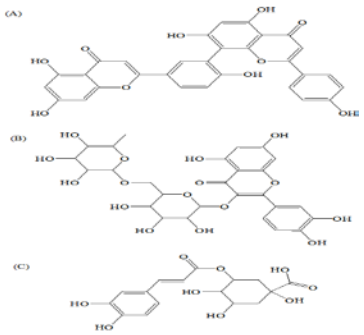

Figure 9. The chemical structure of (A) amentoflavone (B) rutin (C) chlorogenic acid.

Table 2 shows the chemical properties of the ligands. The predicted ADME profiles, namely absorption, distribution, metabolism, elimination were computed by Swiss ADME, and are presented in Table 3. Swiss ADME shows that the three compounds cannot cross the blood-brain barrier, and have low absorption via the human gastrointestinal tract. Only Rutin is a substrate for P-glycoprotein. None of the compounds is inhibitory of the cytochromes. Amentoflavone and rutin show violation of the Lipiniski's rule, since their molecular weights are more than 500, the logP of amentoflavone is greater than five, and rutin has its hydrogen bond acceptors being more than 10. In respect to this rule, chlorogenic acid appears to be better than the other two natural products.

Table 2. Molecular descriptors of the compounds.

Compound	Mass (g/mol)	xlogP	H-bond donors	H-bond acceptors	Polar surface area (Å^2)
Amentoflavone	538.464	5.61	6	10	182
Rutin	610.521	-1.06	10	16	269
Chlorogenic acid	353.303	-0.45	5	9	168
Scutellarin	461.355	0.07	6	12	210
Takakin	300.266	2.74	3	6	100
Coumestrol	268.224	2.54	2	5	84
Hinokinin	354.358	3.02	0	6	63
Bucegin	314.293	3.02	2	6	89
Isoquercitrin	464.379	-0.36	8	12	211
Vitexin	432.381	0.52	7	10	181

Table 3. Swiss ADME predicted pharmacokinetics of the ligands.

Compound	GI absorption	BBB permeant	P-gp substrate	CYP 450 Inhibition				
				CYP1A2	CYP2C19	CYP 2C9	CYP2D6	CYP 3A4
Amentoflavone	Low	No	No	No	No	No	No	No
Rutin	Low	No	Yes	No	No	No	No	No
Chlorogenic acid	Low	No	No	No	No	No	No	No
Scutellarin	Low	No	Yes	No	No	No	No	No
Takakin	High	No	No	Yes	No	Yes	Yes	Yes
Coumestrol	High	No	No	Yes	No	No	Yes	No
Hinokinin	High	Yes	No	Yes	Yes	Yes	Yes	Yes
Bucegin	High	No	No	Yes	No	Yes	Yes	Yes
Isoquercitrin	Low	No	No	No	No	No	No	No
Vitexin	Low	No	No	No	No	No	No	No

4. Discussion

The actin-like protein MreB regulates the synthesis of the cell wall. The length and number of polymer and its curvature are correlated to the cell width and cylindrical uniformity of the cell (Bratton *et al*., 2018). The anionic phospholipids, phosphatidylglycerol and cardiolipin are essential to MreB activity since they would be deposited at the cell poles and an irregular shape is developed due to lack of these phospholipids (Kawazura *et al*., 2017). Van den Ent *et al.,* (2001) suggested that MreB of *T. maritima* possesses a similar topology to actin. The tertiary structure appears to be composed of two domains (I and II) where a nucleotide-binding site is formed by the cleft between the two domains. Each domain is subdivided into two sub-domains A and B.

Walker *et al.* (1982) suggested that an ATP-binding motif, also called Walker A, having the sequence of $GX_4GK[S/T]$, is found in the nucleotide recognition sequences of many proteins (Walker *et al.*, 1982). Several Walker-A sequence variants have been identified; for example, the serine/threonine residue may be replaced by aspartic acid or glycine in some kinases. Several proteins that bind ATP may also have G-rich loops, GXGXXG, which bind the α and β phosphates of ATP (Bossemeyer, 1994; Leipe *et al.*, 2003). A second sequence, the Walker-B motif, contains a conserved aspartic or glutamic-acid residue which is preceded by four hydrophobic residues. This second motif forms coordinate bonds with the Mg^{2+} ion which is necessary for the catalysis of the ATPase reaction (Walker *et al.*, 1982). However, Bork *et al.*, (1992) suggested that MreB and its related division protein, FtsA, contain two ATP binding motifs one for phosphate: V^{163}, V^{164}, D^{165}, I^{166}, G^{167}, G^{168}, G^{169} and T^{170}, and a second for adenosine: V^{292}, L^{293}, T^{294}, G^{295} and G^{296}.

Although many online automated servers have been developed for homology modeling, reliability and accuracy of these models for docking experiments should be explored and assessed. ERRAT is a statistical potential to detect regions of errors the basis of heavy atomic-pair distributions (CC, CN, CO, NN, NO and OO) of the amino-acid residues that are compared with a set of 96 experimental structures. A high-resolution experimental structure usually produces quality factors of 95 % or higher, but those had a lower resolution showing an average of 91 % as a quality factor (Colovos and Yeates, 1993). PROSA is another statistical potential method to measure the energy difference in terms of standard deviation between a native fold of protein and an ensemble of alternative folds to predict error in the constructed model. The energy of the model is shown against the known X-ray and the NMR solved structures of proteins deposited in the Protein Data Bank (Zhang and Skolnick, 1992; Wiederstein and Sippl, 2007).

QMEAN6 estimates the quality of the models by six indices. These are (a) the solvation potential, (b) the torsion angle potential, (c) two distance-dependent potentials: one based on β-atoms, and the second is based on all-atom, and (d) two terms: one compares the predicted secondary structure with a computed (SSE agree.), and the second is for the solvent accessibility (ACC agree.) (Benkert *et al.*, 2009, 2011). In the Ramachandran plot analysis, normally 98.0 % of the residues are expected to be in the favored region, and 2 % are in the allowed region for accurate models (Lovell *et al.*, 2002).

Amentofalvone is a bioflavonoid extracted from *Selaginella tamariscina*. It has an antibacterial action and possesses a synergistic effect with antibiotics (ampicillin, cefotaxime and chloramphenicol) when tested on *Staphylococcus aureus*, *Enterococcus faecium*, *E. coli* and *Pseudomonas aeruginosa* (Hwang *et al*., 2013). Moreover, Kaikabo *et al*. (2009) had isolated amentoflavone from *Garcinia livingstonei*, and suggested that it has an antibacterial activity against *S. aureus*, *E. faecalis*, *E. coli*, and *P. aeruginosa*.

Rutin is 3, 4, 4', 5, 7-pentahydroxyflavone-3-rhamnoglucoside, a flavonoid present in tea, apples and onions with many medicinal activities such as antifungal, antibacterial and anti-cancer potentials (Sharma *et al*., 2013; Janbaz, 2002).

Chlorogenic acid is a polyphenolic compound found in apricots where its methanolic extract, containing 968.125 µg/ml of the compound, inhibited *E. coli*, *Salmonella entritidis* and *Helicobacter pylori* (Mujtaba *et al*., 2017). Lou *et al.* (2011) suggested that chlorogenic acid has antimicrobial activities against bacteria at minimum inhibitory concentrations ranging between 20-80 µg/ml. A possible mechanism of its action is the disruption of the plasma membrane which becomes permeable to cytoplasmic components including nucleotides.

Lipinski *et al.,* (2001) suggested a rule of five to predict the solubility and permeability of a candidate drug. In this rule, poor permeability probably occurs when there are more than five hydrogen bond donors, ten hydrogen bond acceptors, and when the molecular weight is greater than five-hundred, and the calculated Log P (logarithm of octanol-water partition coefficient) is greater than five. The polar surface area also estimates a drug's permeability. Compounds with a polar surface area being greater than 140 $Å^2$ may have poor permeability across cell membranes, and for crossing the blood-brain barrier, compounds need to have a polar surface area less than 90 $Å^2$ (Pajouhesh and Lenz, 2005). Lipinski *et al.* (2001) stated that in spite of the fact that a huge amount of compounds were used to predict this rule, several classes of drugs such as antifungal and antibacterial drugs are exceptions. Drugs that are subjected to transporters inside the human body are excluded from the rule as well.

Many factors affect the gastrointestinal tract absorption. Some of these factors are physicochemical such as the solubility and lipophilicity, while others are physiological such as active transport and efflux. The prediction of drug permeability across the blood-brain barrier is necessary when a drug is required to exert a therapeutic effect on the central nervous system, or when adverse effects of a drug in the brain are being questioned (de la Nuez and Rodríguez, 2008).

P-glycoproteins are members of the ATP-binding cassette transporter family and are responsible for multiple-drug resistance. By their efflux, P-glycoproteins decrease the bioavailability of a drug by reducing its levels inside human cells (Lin, 2003; van de Waterbreemd and Gifford, 2003). P-glycoproteins are found on the surface of biliary canalicular hepatocytes, the luminal surface of epithelial cells of the gastrointestinal tract, the proximal convoluted tubular cells of the kidney, and the capillary endothelial cells of the blood-brain barrier (Thiebut *et al.*,,

1987). The human CYP isoforms CYP3A4, CYP2C9, CYP2C19 and CYP2D6 account for about 80 % of the oxidative metabolism of drugs, the first stage of elimination (Williams *et al*., 2004).

In the pharmaceutical industry, the chemical and physical modifications of the parent compounds are implemented to enhance their properties including solubility and absorption, e.g. nanosuspension, solid dispersions, use of carriers and surfactants, and the reduction of particle size (Chaudry and Patel, 2013). Upretti *et al.* (2011) suggested adding a terpene glycoiside and cyclodextrin to increase the solubility of drugs.

5. Conclusion

The bioinformatics' tools, including homology modeling and docking, may be implemented in the preliminary screening of drugs. The three compounds identified above may be capable of binding the active site of MreB, and may interfere with its ATPase activity. Amentoflavone, rutin, and chlorogenic acid can be useful as lead compounds to target MreB in *E. coli* and other bacilli affecting humans; however, in vitro and animal studies should be carried out to elucidate their effects. Pharmacokinetics and pharmacodynamics are essential in the drug discovery process. The pharmacological properties could be improved by the chemical and physical modifications of the drugs.

References

Allsop A and Illingworth R. 2002. The impact of genomics and related technologies on the search for new antibiotics. *J Appl Microbiol*., **92:**7-11.

Bendezú FO and de Boer PA. 2008. Conditional lethality, division defects, membrane involution, and endocytosis in *mre* and *mrd* shape mutants of *Escherichia coli*. *J Bacteriol*., **190:** 1792-1811.

Benkert P, Biasini M and Schwede T. 2011. Toward the estimation of the absolute quality of individual protein structure models. *Bioinformatics*, **27(3):** 343-350.

Benkert P, Kunzli M and Schwede T. 2009. QMEAN server for protein model quality estimation. *Nucleic Acids Res*., **37:** W510-W514.

Bork P, Sander C and Valencia A. 1992. An ATPase domain common to prokaryotic cell cycle proteins, sugar kinases, actin and hsp70 heat shock proteins. *Proc Natl Acad Sci USA*, **89:**7290-7294.

Bossemeyer D. 1994. The glycine-rich sequence of protein kinases: A multifunctional element. *Trends Biochem Sci*., **19:**201-205.

Bratton BP, Shaevitz JW, Gitai Z and Morgenstein RM. 2018. MreB polymers and curvature localization are enhanced by RodZ and predict *E. coli*'s cylindrical uniformity. *Nat Commun.* **9(1):**2797.

Castrignano T, De Meo PD, Cozzetto D, Talamo IG and Tramontano A. 2006. The PMDB protein model database. *Nucleic Acids Res*., **34(1):** D306-309.

Chaudry VB and Patel JK. 2013. Cyclodextrin inclusion complex to enhance solubility of poorly water soluble drugs: A review. *Inter J Pharma Sci Res.* **4(1):**68-76.

Colavin A, Shi H and Huang KC. 2018. RodZ modulates geometric localization of the bacterial actin MreB to regulate cell shape. *Nat Commun*. **9(1):**1280.

Colovos C and Yeates TO. 1993. Verification of protein structures: Patterns of non-bonded atomic interactions. *Protein Sci*., **2:**1511-1519.

Daina A, Michielin O and Zoete V. 2017. SwissADME: A free web tool to evaluate pharmacokinetics, drug-likeness and medicinal chemistry friendliness of small molecules. *Sci Rep.*, **7:**42717.

de la Nuez A and Rodríguez R. 2008. Current methodology for the assessment of ADME-Tox properties on drug candidate molecules. *Biotec Aplic*., **25(2):** 97-110.

Doi M, Wachi M, Ishino F, Tomioka S, Ito M, Sakagami Y, Suzuki A and Matsuhashi M. 1988. Determinations of the DNA sequence of the *mreB* gene and of the gene products of the mre region that function in formation of the rod shape of *Escherichia coli* cells. *J Bacteriol*., **170:**4619-4624.

Hall TA. 1999. BioEdit: A user-friendly biological sequence alignment editor and analysis program for Windows 95/98/NT. *Nucl Acids Symp Ser*., **41:**95-98.

Huang S-Y and Zou X. 2010. Advances and challenges in protein-ligand docking. *Inter J Mol Sci*., **11:**3016-3034.

Hwang JH, Choi H, Woo E-R and Lee DG. 2013. Antibacterial effect of amentoflavone and its synergistic effect with antibiotics. *J Microbiol Biotechnol*., **23(7):**953-958.

Kaikabo AA, Samuel BB, Eloff JN. 2009. Isolation and activity of two antibacterial biflavonoids from leaf extracts of *Garcinia livingstonei* (Clusiaceae). *Nat Prod Commun.* **4(10):**1363-1366.

Kawazura T, Matsumoto K, Kojiima K, Kato F, kanai T, Niki H and Shiomi D. 2017. Exclusion of assembled MreB by anionic phospholipids at cell poles confers cell polarity for bidirectional growth. *Mol Microbiol.* **104(3):**472-486.

Irwin JJ, Sterling T, Michael MM, Bolstad ES and Coleman RG. 2012. ZINC: A free tool to discover chemistry for biology. *J Chem Inf Model*., **52:**1757-1768.

Iwai N, Nagai K and Wachi M. 2002. Novel S-bezylsiothiourea compound that induces spherical cells in *Escherichia coli* probably by acting on a rod-shaped-determining protein(s) other than penicillin-binding protein 2. *Biosci Biotechnol Biochem.*, **66:**2658-2662.

Janbaz KH, Saeed SA and Gilani AH. 2002. Protective effect of rutin on paracetamol- and CCl4-induced hepatotoxicity in rodents. *Fitoterapia.*, **37:**557-563.

Jones LJF, Carballido-Lopez R and Errington J. 2001. Control of cell shape in bacteria: helical, actin-like filaments in *Bacillus subtilis*. *Cell*, **104:**913-922.

Källberg M, Wang H, Wang S, Peng J, Wang Z, Lu H and Xu J. 2012. Template-based protein structure modeling using the RaptorX web server. *Nat Protocols*, **7:**1511-1522.

Kim S, Thiessen PA, Bolton EE, Chen J, Fu G, Gindulyte A, Han L, He J, He S, Shoemaker BA, Wang J, Yu B, Zhang J and Bryant SH. 2016. PubChem substance and compound databases. *Nucleic Acid Res*., **44:** D1212-1213.

Leipe DD, Koonin EV and Aravind L. 2003. Evolution and classification of P-loop kinases and related proteins. *J Mol Biol*., **333**:781-815.

Lin JH. 2003. Drug-drug interaction mediated by inhibition and induction of P-glycoprotein. *Adv Drug Deliv Rev*., **55:** 53-81.

Lipinski CA, Lombardo F, Dominy BW and Feeney PJ. 2001. Experimental and computational approaches to estimate solubility and permeability in drug discovery and development settings. *Adv Drug Delivery Rev*., **46:**3-26.

Lou Z, Wang H, Zhu S, Ma C and Wang Z. 2011. Antibacterial activity and mechanism of action of chlorogenic acid. *J Food Sci*., **76**: M398-403.

Lovell SC, Davis IW, Arendall 3rd WB, de Bakker PI, Word JM, Prisant MG, Richardson JS and Richardson DC. 2003. Structure validation by Cα geometry: Phi, psi and Cβ deviation. *Proteins: Struct Funct Genet.*, **50(3):**437-450.

Lowe J and van den Ent F. 2014. Bacterial actin MreB forms antiparallel double filaments. *Elife*, **3:**2634.

Mujtaba A, Masud T, Ahmed A, Ahmed W, Jabbar S and Levin RE. 2017. Antibacterial activity by chlorogenic acid isolated through resin from apricot (*Prunus Armeniaca* L.). *Pakistan J Agric Res*., **30(2)**:144-148.s

Pajouhesh H and Lenz GR. 2005. Medicinal chemical properties of successful central nervous system drugs. *Neuro Rx*, **2(4):**541-553.

Salje J, van den Ent F, de Boer P and Löwe J. 2011. Direct membrane binding by bacterial actin MreB. *Mol Cell*, **43:**478-487.

Sharma S, Ali A, Ali J, Sahni JK and Baboota S. 2013. Rutin: Therapeutic potential and recent advances in drug delivery. *Expert Opin Investig Drugs*, **22:**1063-1079.

Sippl MJ. 1993. Recognition of errors in three-dimensional structures of proteins. *Proteins*, **17:**355-362.

Slovak PM, Porter SL and Armitage JP. 2006. Differential localization of Mre proteins with PBP2 in *Rhodobacter sphaeroides*. *J Bacteriol*., **188:**1691-1700.

Thiebut F, Tsuruo T, Hamada H, Gottesman MM and Pastan I. 1987. Cellular localization of the multidrug resistance gene product P-glycoprotein in normal human tissues. *Proc Natl Acad Sci USA*, **84:**7735-7738.

Thompson M. 2004. ArgusLab 4.0.1. Planaria Software LLC. Available at (http://www.arguslab.com). Seattle, Washington, USA.

Trott O and Olson AJ. 2010. AutoDock Vina: Improving the speed and accuracy of docking with a new scoring function, efficient optimization and multithreading. *J Comput Chem*., **31(2):**455-461.

Upreti M, Prakash I and Chen YL. 2011. Solubility enhanced terpene glycosides(s). PCT/US2011/02436.

van de Waterbeemd H and Gifford E. 2003. ADMET *in silico* modeling: Towards prediction paradise? *Nature*, **2:**192-204.

van den Ent F, Johnson CM, Persons L, de Boer P and Löwe J. 2010. Bacterial actin MreB assembles in complex with cell shape protein RodZ. *EMBO J*., **29:** 1081-1090.

van den Ent V, Amos LA and Löwe J. 2001. Prokaryotic origin of the actin cytoskeleton. *Nature*, **413(6):**39-44.

Wachi M, Doi M, Okada Y and Matsuhashi M. 1989. New *mre* genes *mreC* and *mreD*, responsible for formation of the rod shape of *Escherichia coli* cells. *J Bacteriol.*, **171:**6511-6516

Wachi M, Doi M, Tamaki S, Park W, Nakajima-Iijima S and Matsuhashi M. 1987. Mutant isolation and molecular cloning of *mre* genes, which determine cell shape, sensitivity to mecillinam, and amount of penicillin-binding proteins in *Escherichia coli*. *J Bacteriol*., **169:**4935-4940.

Walker JE, Saraste M, Runswick M and Gay NJ. 1982. Distantly related sequences in the alpha- and beta-subunits of ATP synthase, myosin, kinases and other ATP-requiring enzymes and a common nucleotide binding fold. *EMBO J*., **1:**945-951.

Wallace AC, Laskowaski RA and Thornton JM. 1996. LIGPLOT: A program to generate schematic diagrams of protein-ligand interactions. *Protein Eng*. **8:**127-134.

Wiederstein M and Sippl MJ. 2007. ProSA-web: Interactive web service for the recognition of errors in three-dimensional structures of proteins. *Nucleic Acids Res.*, **35:**W407-410.

Williams JA, Hyland R, Jones BC, Smith DA, Hurst S, Goosen TC, Peterkin V, Koup JR and Ball SE. 2004. Drug-drug interactions for UDP-glucuronosyltransferase substrates: A pharmacokinetic explanation for typically observed low exposure (AUCi/AUC) ratios. *Drug Metab. Dispos.*, **32**:1201-1208.

Zhang L and Skolnick J. 1992. What should the Z-score of native structure be? *Protein Sci*., **7:**1201-1207.